ISSN 1392–1207. MECHANIKA. 2022 Volume 28(6): 455–461

Helical Baffle Thermohydraulic Performance Versus Segmental Baffle One

Mahdia YOUSFI
20 août 1955 University of Skikda, Skikda 21000, Algeria, E-mail: m.youcefi@univ-skikda.dz
crossref http://dx.doi.org/10.5755/j02.mech.31096

1. Introduction

Baffles, in shell-and-tube heat exchangers (STHXs), play a vital role and are continually subject of investigations, their shape and arrangement are of essential importance for the thermohydraulic performance. The segmental baffles still remain the most commonly used in STHXs due to their robustness, easy maintenance, and ability to enhance turbulence and local mixing on the shell side. However, straight baffles generate major drawbacks such as: large shell-side pressure drop, dead zone between two adjacent baffles which would increase the fouling resistance, and high risk of vibration failure on tube bundle. To overcome these shortcomings, a number of improved structures was stood up, and Lutcha and Nemcansky [1] were the first ones who proposed helical baffles in 1990. They found that, for all tested helical inclination angles, at equal pressure drop, the helical baffles produced higher heat transfer coefficients than segmental ones, and that 40° inclination gave the highest coefficient which was almost twice as large as that for an equivalent segmental baffles. Since them, different configurations have been suggested, such as continuous helical baffles, discontinuous helical baffles, combined helical baffles and trisection helical baffles [2-4]. Stehlik et al. [5], under turbulent flow, starting from inclination angle of 25° (18° under laminar regime) up to an optimal, observed (1) a postulated flow instability development that enhanced turbulence and heat transfer, the latter at the maximum helix angle of 42° was 1.39 times than for ideal cross-flow conditions; (2) a decrease in pressure drop, ranged from a factor of 0.26 to a maximum of 0.6 at an inclination angle of 45°. Kral et al. [6] performed tests on units with various baffle geometries, they found that the helical baffles provided much higher efficiency compared to conventional segmental baffles, when pressure drop plotted against heat transfer rate, and that a helix angle of 40° was an optimal.

In his experimental study, Shuli [7] showed that the greater the inclination angle of the baffles the lower the pressure drop for a given mass flow, and for each helix angle the minimum pressure drop occurred at a certain Reynolds number which shifted up as the angle increased. Nemati et al. [8] presented a numerical simulation of continuous and non-continuous helical baffles at a helix angle of 40°; they found that: 1. For a fixed flow rate, the longer the space between two adjacent baffles, the lower the heat transfer coefficient; 2. For a fixed pressure gradient, the larger the space between two adjacent baffles, the higher the heat transfer coefficient, the continuous helical baffles gave them the best performance. Also, numerically. Zhang et al. [2] tested different shapes of helical baffle and established that 1. Quarter-sector helical baffles had the lowest pressure drop at 10° and 20°; 2. Quarter-sector helical baffles had the best ratio transfer coefficient of heat to pressure loss, although at 30° the ratio for quarter-sector helical baffles was almost the same as for quarter-ellipse helical baffles; 3. Heat transfer coefficient and pressure drop decreased as helix angle and mass flow increased. When Gao et al [9] increased the helix angle in their experimental study, they observed an increase in the heat transfer coefficient per unit pressure drop for a given volume flow rate and they proposed, in case of adapting an existing SB-STHX to helical baffles, small baffle helix angles with the condition of low Reynolds number. Shinde and Chavan [10] carried out experiments on fiber-reinforced plastic helical baffles at a helix angle of 25°, obtained better performance compared to segmental baffles and proposed fiber-reinforced plastic as a replacement for baffle conventional material because the deviation from the heat transfer coefficient was in the range of 8% to 10%; they also done numerical study and found when they increased the helix angle that the ratio of heat transfer to pressure drop increased to a maximum at 21° and then dropped.

In short, helical baffles are still considered new technology being used to improve the thermohydraulic performance of STHXs. Although numerous experimental and numerical studies had investigated whether the effectiveness of HB-STHX is greater or less than that of SB-STHX, and reviews of major works were provided to show that they can be advantageous [11], this remains to be clarified. The current study is intended as a quick check tool, framed solely by the Delaware technique. The schematic flow pattern is analyzed as in Tinker's analysis [12] and the effect of streams are as established in Stehlik et al. experimental investigation [5], but bypass correction factors for heat transfer coefficient and pressure drop were slightly modified to consider a novel stream specific to helical baffles highlighted in CFD surveys [13, 14].

2. Mathematical modelling

In industry, it seems that the most adopted helical baffle cycle is the four-circular continuous sector-shaped plates arranged in a pseudo-helical manner. Each baffle occupies one quadrant of the exchanger shell cross-section. We talk about continuous connection when two adjacent baffles joined end to end at the perimeter of each sector, and so forming a continuous helix at the outer periphery (Fig. 1), while overlapped (or discontinuous) connection is when two adjacent helical baffles touch the perimeter of each other. In non-continuous helical baffles, the overlap proportion e is defined as $e = (2l/D_s) \times 100\%$ where D_s is the shell inside diameter; l is the length from the shell inner wall to the touch point of two adjacent baffles. When $e = 50\%$, we say a middle-overlap baffles, while for continuous baffles $e = 0$

($l = 0$). A crucial parameter so-called helix or inclination angle is the angle φ between normal line to the circular sector-shaped plate and the axis of the helical heat exchanger and which is related to the helical pitch, the period of the pseudo-spiral.

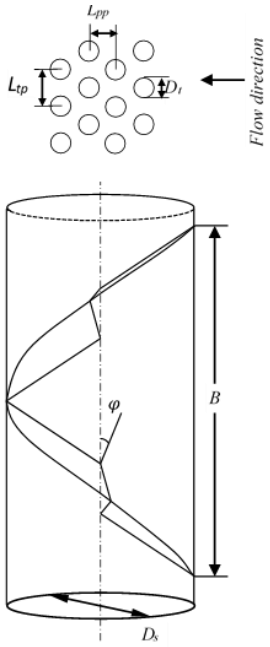

Fig. 1 Schematics of parameter definition of continuous HB-STHX

Despite helical baffled shell-side flow paths might be more complex than the segmental ones, as the quarter-sectors force the fluid to move in a pseudo-helical path across the bundle nest, the schematic flow pattern (Fig. 2) is analyzed similarly to the model originally proposed by Tinker [11] and later modified by Palen et al. [15]. Thus, due to the flow resistances through clearances, the helical shell-side flow is divided into six separate partial streams.

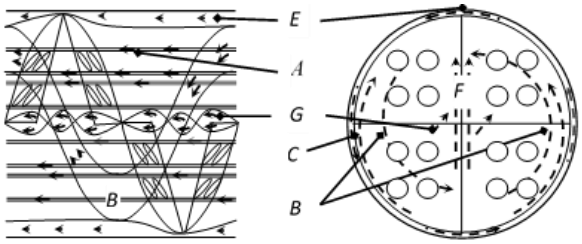

Fig. 2 Shell-side flow pattern in HB-STHX

We have an effective main cross-flow stream for both heat transfer and pressure drop, Stream B, which is related to flow across ideal tube banks. There are two stream leakages, Stream *A* and Stream *E*. Stream *A* occurs through the diametral clearance between the baffle tube hole and the outside tube wall, as it flows nearby outside tube walls it is not detrimental to heat transfer. Stream *E* exists between successive quarter-sector edges and the inside shell wall, this stream is the most undesirable one for heat transfer, particularly in laminar flow, because it does not exchange heat with any tubes. There are also two bypass streams, Stream *C* and Stream *F*. Stream *C* takes place through the annular gap between the bundle and the inside shell wall, and is partially ineffective for heat transfer as it exchanges heat only with periphery tubes of the bundle. Stream *F* is present only in some tube layouts, due to open passages in tube pass partitions in multi-pass units, as it comes into contact with less tube wall area, this stream is less unfavorable than the stream *C* but more unfavorable than stream *A*. The sixth flow, observed in CFD studies [11, 12], specific to HB-STHX, the *G* Stream, has to be added and could be considered as bypass type. It seems obvious that it takes place, because the pseudo-spiral arrangement of the quarter baffles delivers a path along the axis of the exchanger that certain fluid particles seem prefer to borrow instead to turn with the main pseudo-spiral. It is undesirable for pressure loss and for heat transfer especially when the baffle tilt is significant, to minimize this stream, sealing strips have to be fitted to block it and force the fluid to return to the main Stream *B*.

2.1. Overall shell-side heat transfer coefficient

The overall shell-side heat transfer coefficient U_0 based on the outside tubes area A_0, without any fouling and for negligible tube curvature, is equal to:

$$\frac{1}{U_0} = \frac{1}{\alpha_s} + \frac{1}{\alpha_t}\left(\frac{D_t}{D_t - 2L_{tw}}\right) + \frac{L_{tw}}{\lambda_{tw}}, \tag{1}$$

where: α_s is the effective shell-side heat transfer coefficient; α_t the tube-side heat transfer coefficient; D_t the tube outside diameter; L_{tw} the tube wall thickness and λ_{tw} the tube wall thermal conductivity which is considered constant as all the thermophysical properties we are using.

α_s is obtained by modifying α_i the ideal shell-side heat rate, as the cited-earlier bypass and leakage flows diminish the latter and their effects on it are expressed by mean of heat transfer correction J factors (defined in Sec. 2.3) that account for : bundle bypass J_b, adverse temperature gradient in laminar flow J_r ($J_r = 1$ for turbulent regime), unequal baffle spacing at inlet and outlet J_s, change in the cross-flow characteristics J_f, and turbulence enhancement J_t [5]. The effective shell-side heat transfer coefficient is then:

$$\alpha_s = \alpha_i \cdot J_b \cdot J_r \cdot J_s \cdot J_f \cdot J_t, \tag{2}$$

the combined effect of correction factors $J_{tot} = J_b \cdot J_r \cdot J_s \cdot J_f$ J_t has to be around 0.6 in a well-designed HB-STHX as it is in SB-STHX [16] which is for the latter $J_{tot} = J_b \cdot J_r \cdot J_s \cdot J_l \cdot J_c$ where J_l a ccounts for baffle leakages and J_c accounts for segmental baffle window. J_c and J_l are not in Eq. (2) since the first one exclusively considers the segmental baffle cut and in the second one, the ratio of the total leakage area per baffle against the cross-flow area between two adjacent segmental baffles weights more heavily in SB-STHX than in HB-STHX where it is insignificant in the way the helical baffles are inclined quarter-sectors.

2.2. Total shell-side pressure drops

The ideal shell-side heat coefficient α_i is calculated from the ideal Colburn J_i factor based on the Stanton number consistent with the Delaware work which is given by [16, 17]:

$$J_i = \frac{\alpha_i}{\left(c_p\right)_s \dot{m}_s}\left(Pr\right)_s^{0.67}\left(\phi_s\right)^{-0.14}, \tag{3}$$

where: $\left(c_p\right)_s$ is the shell-side fluid specific heat; $\dot{m}_s$ is the mass velocity; the ratio of $\dot{M}_s$ is the mass flow rate on the shell-side against S_m the cross-sectional minimum area at the shell centerline defined in Eq. (4); ϕ_s is the Sider-Tate correction factor; the ratio of η_s the dynamic viscosity at shell-side bulk average temperature versus the dynamic viscosity at tube wall temperature.

Table 1

Thermophisical properties

Shell-side inlet temperature, °C	70
Tube-side temperature, °C	40
Shell-side outlet temperature, °C	55
Shell-side viscosity, cP	0.429
Shell-side density, kg/m^3	998.2
Shell-side heat capacity, J/kg K	4182
Shell-side thermal conductivity, W/m K	0.6
Tube-wall thermal conductivity, W/m K	40
Shell-side mass flow rate, kg/s	10, 13, 17, 22, 25, 30

In Eq. (3), the ratio $\alpha_i \big/ \left(c_p\right)_s \dot{m}_s$ represents *St* the Stanton number known as Nu_s / ($Re_s \cdot Pr_s$) where Nu_s, Re_s and Pr_s is the Nusselt, Reynolds and Prandtl number respectively. All these numbers are defined for shell-side fluid with reference velocity based on S_m and characteristic length: the outside tube diameter.

The cross-sectional minimum area S_m at the shell centerline for HB-STHX is calculated according to [5]:

$$S_m = 0.5B\left[D_s - D_{otl} + \frac{D_{otl} - D_t}{L_{tp,eff}}\left(L_{tp} - D_t\right)\right], \tag{4}$$

where: D_{otl} is the tube bundle-circumscribed circle; L_{tp} denotes the tube layout pitch and $L_{tp,eff}$ is the tube pitch perpendicular to flow direction. The term B represents the helical pitch (cycle amplitude) which depends on: the baffle helix angle φ, the baffle overlaps proportion e, the number of baffles per cycle N_b and the shell inside diameter D_s, as defined in below [9, 18, 19]:

$$B = \left(1-e\right)N_b D_s \sin\left(\frac{\pi}{N_b}\right)\tan\left(\varphi\right), \tag{5}$$

where: $N_b \geq 2$ and $0 \leq e < 1$, in the case of four quadrant sector continuous helical baffles, we get $B = 2\sqrt{2}D_s \tan\left(\varphi\right)$ [18]. For SB-STHX, S_m is written as in Eq. (4) but replacing $0.5B$ by L_{bc}: the central baffle spacing.

The multiple undesirable streams cited earlier effects also the ideal tube bank-based pressure loss known as [16, 17]:

$$\Delta p_{bi} = f_i\left(\frac{2\dot{m}_s^2}{\rho_s}\right)N_{tcc}\left(\phi_s\right)^{-0.14}, \tag{6}$$

where: f_i is the ideal tube bank friction factor; ρ_s the shell-side fluid density and N_{tcc} the number of effective crossed tube rows. For four quadrant sector continuous helical baffles, we have $N_{tcc} = D_s / L_{pp}$; L_{pp} is the perpendicular tube layout pitch (Fig. 1).

The total shell-side pressure drops Δp_s, in HB-STHX, is the sum of only two distinct parts; Δp_c the pressure loss in the cross flow per cycle and Δp_e the pressure drops in the baffle end zones [5]:

$$\Delta p_c = \Delta p_{bi}\left(\frac{L_{ta}}{B}\right)R_b \cdot R_f \cdot R_t, \tag{7}$$

$$\Delta p_e = \Delta p_{bi} R_s \cdot R_f \cdot R_t, \tag{8}$$

where: L_{ta} is the baffled length of the tube bundle. R_b, R_s, R_f and R_t are correction factors of the ideal pressure drop (defined next) that consider the same effects as those of correction J factors with same subscript. In SB-STHX, a third pressure loss Δp_w is to add, to account for pressure drop in all segmental baffle windows crossed.

2.3. Correction factors

To estimate all the correction factors involved in the HB-STHX case, we have used the Zhang et al. [17] equations fitted to Stehlik et al. [5] curves, but we have not kept the same symbols for sake of convenience as we took from the start Schlunder [16] as a reference for symbol notation. So, for the bypass effect factors, we have:

$$J_b = exp\left\{-1.343F_{sbp}\left[1-\left(2r_{ss}\right)^{0.338}\right]\right\}, \tag{9}$$

$$R_b = exp\left\{-3.56F_{sbp}\left[1-\left(2r_{ss}\right)^{0.363}\right]\right\}, \tag{10}$$

where: F_{sbp} is the fraction of the bypass area S_b as defined below in Eq. (11), against the overall cross-flow area S_m (Eq. (4)); r_{ss} is the ratio of N_{ss} the number of sealing strips pairs in one baffle cycle versus N_{tcc}. The bypass area is given by:

$$S_b = 0.5B\left(D_s - D_{otl} + L_{pl}\right), \tag{11}$$

where: L_{pl} expresses the effect of the tube lane partition bypass width which equals zero for all standard calculations but $Dt/2$ for estimation purposes [16].

To consider the bypass G Stream, it is necessary to add a bypass area S_{bc} to the side of S_b in the numerator of F_{sbp} fraction to express the passage section of the infective longitudinal flow at the level of the centerline. S_{bc} is closely related to the inclination angle of the baffles: greater the angle, larger this area, more sealing strips are required. Thus, in HB-TSHXs, it is not only the tubesheet type that imposes sealing but also the size of S_{bc}, we estimate that if the latter exceeds the value $0.115B$, N_{ss} must not be zero. As there isn't yet formula for the G Stream effect, we propose to modify the Stehlik factors J_b and R_b by multiplying them by $exp\left(-1.21\varphi/360\right)$ and $exp\left(-3.20\varphi/360\right)$ respectively to weight the influence of this bypass flow, hence the modified factors are:

$$J_{bM} = exp\left\{-1.21\frac{\varphi}{360} - 1.343F_{sbp}\left[1-\left(2r_{ss}\right)^{0.338}\right]\right\}, \tag{12}$$

$$R_{bM} = exp\left\{-3.20\frac{\varphi}{360} - 3.56F_{sbp}\left[1-\left(2r_{ss}\right)^{0.363}\right]\right\}. \quad (13)$$

For the unequal end spacing effect factors, we get:

$$J_s = 1.079\left(\frac{B}{D_s}\right)^{0.0487} - 0.445\left(\frac{B}{D_s}\right)^{-0.301}\left(\frac{L_{bo}+L_{bi}}{L_{ta}}\right)^{1.2}, \quad (14)$$

$$R_s = \left[-0.0172 + 0.0899\left(\frac{B}{D_s}\right)\right]\left(\frac{L_{bo}+L_{bi}}{L_{ta}}\right)^{-1.2}, \quad (15)$$

where: L_{bi} and L_{bo} are the inlet and outlet non-baffled spacing, in HB-STHX.

The change in the cross-flow characteristics effect factors are:

$$J_f = 0.977 + \left(4.55\times10^{-3}\right)\varphi - \left(1.821\times10^{-4}\right)\varphi^2, \quad (16)$$

$$R_f = 0.289 - \left(5.06\times10^{-4}\right)\varphi - \left(4.53\times10^{-5}\right)\varphi^2, \quad (17)$$

and the turbulence enhancement effect factors are:

$$J_t = -56.39 + 8.28\varphi - 0.46\varphi^2 + 0.012\varphi^3 - \\ -\left(1.64\times10^{-4}\right)\varphi^4 + \left(8.19\times10^{-7}\right)\varphi^5, \quad (18)$$

$$R_t = -5.411 + 0.379\varphi - \left(4.02\times10^{-3}\right)\varphi^2. \quad (19)$$

In this work, we are investigating how the thermo-hydraulic performance will be affected when segmental baffles are replaced by helical ones. The Bell–Delaware approach is used and the design procedure is the rating mode which apply for an existing heat exchanger, so all the geometries are fully specified and the task is to obtain the overall heat transfer coefficient and the pressure loss for the shell-side. The summarized steps of the rating procedure are as follows:

1. Define geometry parameters and process conditions;
2. Select baffle inclination φ and overlap ratio e;
3. Compute various flow areas: S_m, S_{bc}, S_b…;
4. Guess primary α_s shell-side heat transfer coefficient;
5. Determine wall temperature;
6. Compute $\dot{m}_s$ the mass velocity and the Re_s Reynolds number;
7. Determine heat transfer J and pressure loss R correction factors;
8. Compute effective α_s shell-side heat transfer coefficient;
9. Repeat steps 5 to 8 until the difference between actual value of α_s and its previous one is reasonable;
10. Determine Δp_s shell-side pressure drop and U_0 global heat transfer coefficient.

3. Results and discussion

The fluid flow conditions and the geometry parameters of our exchanger are presented in Tables 1 and 2. We have chosen liquid water as the shell-side working fluid as well as the tube-side, the latter is considered isothermal with a specified tube-side heat transfer coefficient α_t at 4000 W/m^2 K as the shell-side constitute the predominant flow resistance [16]. The overlap proportion e is taken null as we have considered only the continuous helical baffles. The Reynolds number is calculated from $Re_s = D_t\dot{m}_s/\eta_s$ for six values of $\dot{M}_s$ the shell-side mass flow rate namely: 10, 13, 17 22, 25 and 30 kg/s, for six different values of the baffle inclination angle ranged from 25° up to 45° and for segmental (SB) case, these will result in different range of Re_s.

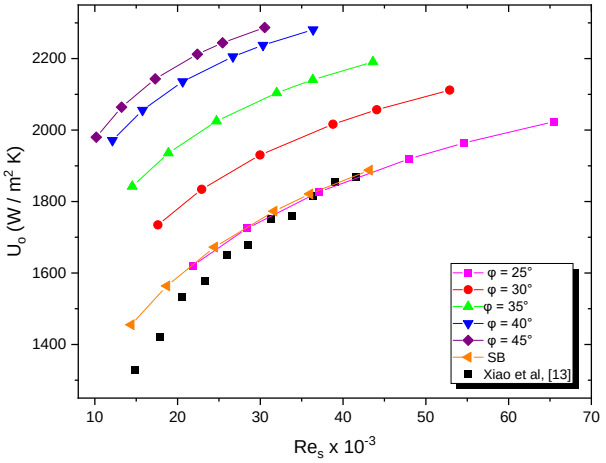

a

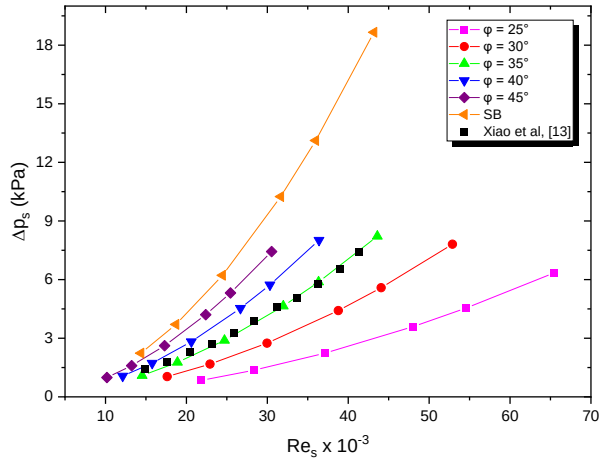

b

Fig. 3 Comparison of a - global heat transfer coefficient, b - shell-side pressure drop, against Reynolds number, between our analytical results and Xiao et al [13] experimental results

In order to validate the reliability of our calculations, comparison of our analytical results with the experimental results of Xiao et al. [13] on a HB-STHX with helix angle of 25°, is shown on Fig. 3, a and b for U_0 the global heat coefficient and Δp_s the pressure loss respectively. It can be seen from these two figures that the trends for both results are similar, they exhibit mainly the same profiles and have nearly the same values, on what we consider that our method in this paper is reliable and applicable.

On Fig. 4, we present the modification that we have made on the correction J_b and R_b factors, the bypass leakage effects on global heat transfer coefficient and pressure drop respectively to consider the additional Stream G effect. We can observe that when the helix angle increase, the modified J_{bM} factor goes down from 0.88 to 0.82 and the modified R_{bM}

factor from 0.71 to 0.60 while the original factors established by Stehlik are relatively constant near 0.96 and 0.89 respectively.

Table 2

Geometry parameter

Shell inside diameter, mm	500
Tube outside diameter, mm	19
Tube effective length, mm	2500
Baffle cut, %	26
Tube layout pattern, °	90
Inlet and outlet non-helical baffled spacing, mm	125
Tube pitch, mm	25
Inside shell-to-baffle diametral clearance, mm	5
Diametral clearance between tube outside diameter and baffle hole, mm	0.8
Helix angle, °	25, 30, 35, 40, 45
Segmental baffle spacing, mm	250
Inside shell diameter-to-tube bundle bypass clearance, mm	10

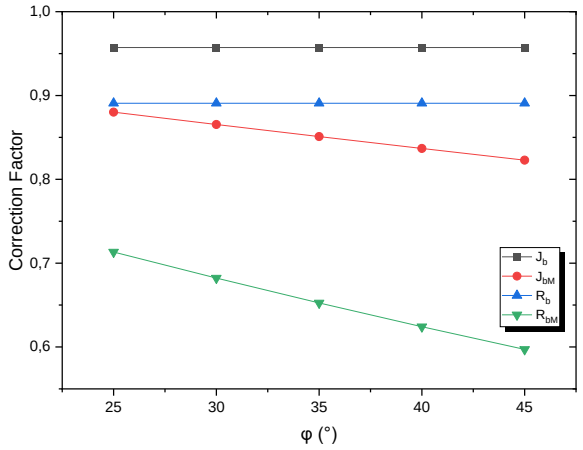

Fig. 4 Variation of modified and Stehlik bundle bypass factors for heat transfer and pressure drop against helix angle

When we examine the global heat transfer coefficient, we notice that it is in positive correlation: with shell-side mass flow rate at a fixed inclination angle (Fig. 3, a) and with inclination angle at a fixed mass flow rate (Fig. 5, a), however the last distribution shows always sharp slow-down growth between the helix angle 40° and 45°. As an example, at 30 kg/s the gain is only 6.03 W/m^2 K between 40° and 45° while is on average 85.76 W/m^2 K between the other angles.

The change in pressure drop with increasing baffle inclination angle follows a somehow parabolic profile at constant mass flow rate (Fig. 5, b) and it increases with increasing mass flow rate at a given inclination angle (Fig. 3, b). Constantly, 25° drives the lowest pressure loss while 35° is the most detrimental to pressure but not more than SBs in which it rises drastically when $\dot{M}_s$ rises (Fig. 3, b). At the highest mass flow rate, we have 18,66 kPa in SB case against 8.23 kPa at 35°.

When Reynolds number goes up, SBs exhibit the almost lowest global heat transfer coefficient (Fig 3, a) and the absolutely highest pressure drop (Fig 3, b) compared to HBs. Inclination angle of 35° is the one to compare with SB case because both have almost the same Re_s (Table 3), this is due to the fact that this inclination angle gives half helical cycle pitch $B/2$ = 247.56 mm very close to L_{bc} = 250 mm the central baffle spacing in SBs (Eq. (4)). Thus, with same turbulence, the zigzagging flow path doesn't enhance heat exchange as pseudo-spiral path does and generates more frictional losses than pseudo-spiral path does.

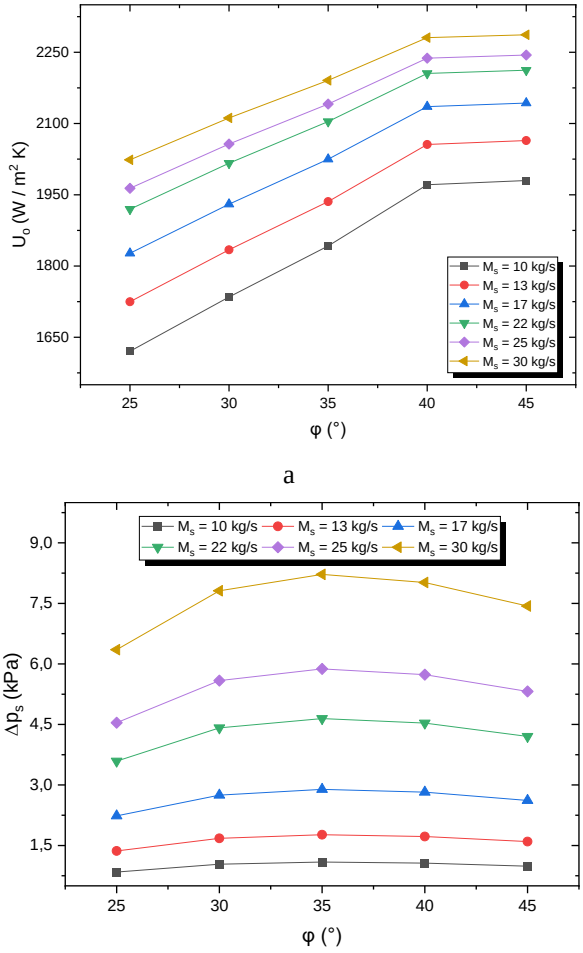

Fig. 5 Variation of a - global heat transfer coefficient, b - pressure loss, against helical baffle inclinations for different values of shell-side mass flow

Table 3

Shell-side Reynolds number values for each helix angle and each mass flow rate

$\dot{M}_s$, kg/s	$Re_s \times 10^{-3}$					
	25°	30°	35°	40°	45°	SB
10	21.826	17.628	14.535	12.129	10.178	14.393
13	28.374	22.917	18.896	15.768	13.231	18.711
17	37.104	29.968	24.710	20.620	17.302	24.469
22	48.017	38.782	31.977	26.684	22.391	31.665
25	54.565	44.071	36.338	30.323	25.444	35.983
30	65.478	52.885	43.606	36.388	30.533	43.180

To analyze the thermohydraulic performance of HB-STHX, it is customary to examine the performance evaluation factor which is the ratio U_s versus Δp_s, as well as to look at each one separately.

We can see on Fig. 6, a that the ratio $U_0 / \Delta p_s$ seems to fall exponentially with increasing mass flow rate at constant baffle inclination, while the decrease is relatively smooth in SB case. For example, between 10 kg/s and 30 kg/s, at inclination of 45°, the ratio drops by

1.70 W/m^2 K kPa with a gradient of 0.085 (W/m^2 K kPa)/(kg/s) and in SB case drops by 0.55 W/m^2 K kPa with a gradient of 0.032 (W/m^2 K kPa)/(kg/s). We also observe that among all plotted cases, SB is the one that displays the lowest thermohydraulic performance ratio.

Low values of mass flow rate give relatively distinct performance ratios for distinct inclinations while high values give nearly the same ratio whatever the angle which is very different from that of SB case (Fig. 6, a). U_0 / Δp_s vary from 2.01 to 1.67 W/m^2 K kPa at $\dot{M}_s = 10$ kg/s and is constantly around 0.30 W/m^2 K kPa at $\dot{M}_s = 30$ kg/s , varying the inclination.

The negative correlation of the performance evaluation factor with turbulence is due to the fact that the pressure drop dominates the heat transfer coefficient and more strongly in the case of helical baffles (as the gradient is higher) when the mass flow rate increases. The convergence, towards a quasi-constant ratio, is explained by the fact that the more the turbulence increases, the more the pressure loss is counterbalanced by the increase in the overall heat exchange coefficient.

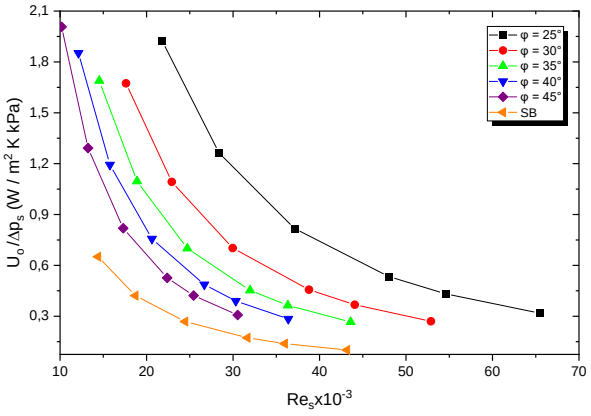

a

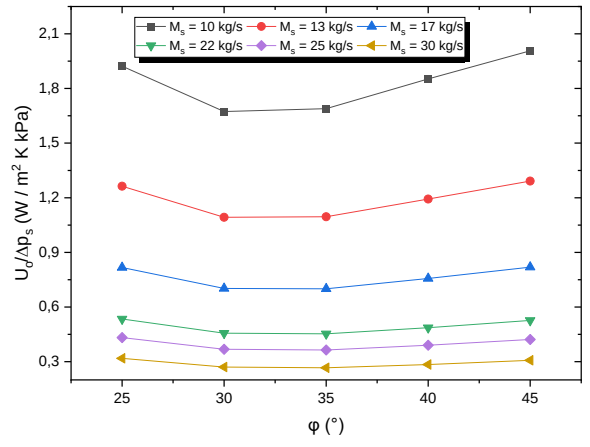

b

Fig. 6 Variation of performance evaluation ratio against a - Reynolds number; b - helical baffle inclination

Fig. 6, b shows a performance ratio in somehow quadratic relation with helix angle. We can see clearly that φ have no significant impact on the ratio U_0 / Δp_s when $\dot{M}_s$ is high, we have almost neglected profile curvature. The influence becomes noticeable only at 17 kg/s and the impact is well marked when it is further smaller (10 kg/s) even though, constantly 45° shows the highest performance evaluation factor followed by 25°. For mass flow rate around 10 kg/s and 13 kg/s, the inclination 30° shows the most disadvantageous ratio U_0 / Δp_s while the angle shifts up to 35° for higher rate, although the values are close.

4. Conclusions

In the current study, a rating design procedure based on Bell-Delaware technique is employed as a quick mean to verify which of the two types HB-STHX and SB-STHX will perform better and which optimum helix angle will be. The helical baffles considered here are continuous quadrant sectors with five different inclination angles from 25° up to 45° and are exanimated at six different values of mass flow in the range of 10 kg/s to 30 kg/s. The major findings drawn are summarized as follows

1. Almost all helix angles performed thermally better than the SB case whatever Reynolds number. 45° helix angle gave 2286.9 W/m^2 K, the highest overall heat transfer coefficient obtained at 30 kg/s, the highest mass flow rate.

2. SBs were by far the most detrimental to pressure drop as turbulence rises. 25° helix angle showed the lowest pressure loss with 0.84 kPa at the lowest mass flow rate 10 kg/s;

3. For higher mass flow rates, the inclination angle did matter little because all the angles converged nearly to a same amount of the performance evaluation factor around 0.30 W/m^2 K kPa which we considered to be quite close to 0.10 W/m^2 K kPa the SB one;

4. When regarding the combined effects of the thermal and hydraulic performances, it was 45° the highest tested inclination angle, that displayed 2.01 W/m^2 K kPa, the best performance evaluation factor, closely followed by 25° with 1.92 W/m^2 K kPa and by far SB case with 0.65 W/m^2 K kPa, all obtained at the lowest mass flow rate;

Consequently, compared to the conventional segmental baffles, continuous helical baffles effectively did increase the heat transfer rate and decrease the pressure drop, rendering a heat exchanger with continuous helical baffles more thermally efficient and consuming less pumping power.

We can recommend HB-TSHXs instead of SB-STHXs for low mass flow rates with: 25° baffle inclination when power pump has to be considered or 45° baffle inclination as a compromise of both performances thermal and hydraulic.

References

1. **Lutcha, J.; Nemcansky J.** 1990. Performance improvement of tubular heat exchangers by helical baffles, Chem. Eng. Res. Des. 68: 263–270.
2. **Zhang, J. F.; He, Y. L.; Tao, W. Q.** 2009. 3D simulation on shell-and-tube heat exchangers with middle-overlapped helical baffles and continuous baffles – Part 1: numerical model and results of whole heat exchanger with middle-overlapped helical baffles, Int. J. Heat Mass Transf. 52: 5371-5380. https://doi.org/10.1016/j.ijheatmasstransfer.2009.07.007.
3. **Zhang, M.; Meng, F.; Geng, Z.** 2015. CFD simulation on shell-and-tube heat exchangers with small angle helical baffles, Front. Chem. Sci. Eng. 9(2): 183-193.

https://doi.org/10.1007/S11705-015-1510-X.
4. **Arani, A. A.; Uosofvand, H.** 2020. Improving shell-and-tube heat exchanger thermohydraulic performance using combined baffles, Int. J. Numer. Method. H. 30 (8): 4119 – 4140. https://doi.org/10.1108/HFF-06-2019-0514.
5. **Stehlik, P.; Němčanský, J.; Kral DSwanson, L. W.** 1994. Comparison of correction factors for shell-and-tube heat exchangers with segmental or helical baffles, Heat Transf. Eng. 15(1): 55–65. https://doi.org/10.1080/01457639408939818.
6. **Kral, D.; Stehlik, P.; Van Der Ploeg, H. J.; I. Master B.** 1996. Helical baffles in shell-and-tube heat exchangers. Part I: experimental verification, Heat Transf. Eng. 17(1): 93–101. https://doi.org/10.1080/01457639608939868.
7. **Shuli, W.** 2002. Hydrodynamic studies on heat exchangers with helical Baffles, Heat Transf. Eng. 23(3): 43–49. https://doi.org/10.1080/014576302753605367.
8. **Nemati, T. F.; Zeyninejad, M. S.; Razmi, K.; Tasouji, A. R.** 2012. Baffle space impact on the performance of helical baffle shell and tube heat exchangers, Appl. Therm. Eng. 44: 143-149. https://doi.org/10.1016/j.applthermaleng.2012.03.042.
9. **Gao, B.; Bi, Q.; Nie, Z.; Wu, J.** 2015. Experimental study of effects of baffle helix angle on shell-side performance of shell-and-tube heat exchangers with discontinuous helical baffles, Exp. Therm. Fluid Sci. 68: 48–57. https://doi.org/10.1016/j.expthermflusci.2015.04.011.
10. **Shinde, S., Chavan, U.** 2018. Numerical and experimental analysis on shell side thermo-hydraulic performance of shell and tube heat exchanger with continuous helical FRP baffles, Therm. Sci. Eng. Prog. 5: 158 -171. https://doi.org/10.1016/j.tsep.2017.11.006.
11. **Salahuddin, U.; Bilal, M.; Ejaz, H.** 2015. A review of advancements made in helical baffles used in shell and tube heat exchangers, Int. Commun. Heat Mass Transf. 67: 104-108. https://doi.org/10.1016/j.icheatmasstransfer.2015.07.005.
12. **Tinker, T.** 1951. Shell-Side characteristic of shell and tube heat exchanger: analysis of the fluid flow pattern and tube heat exchanger and the effect of flow distribution on the heat exchanger performance, Proceedings of Inst. Mech. Eng. and ASME. https://doi.org/10.1115/1.4012245.
13. **Xiao, X. ; Zhang, L. ; Li, X. ; Jiang, B. ; Yang, X. ; Xia, Y**. 2013. Numerical investigation of helical baffles heat exchanger with different Prandtl number fluids, Int. J. Heat Mass Transf. 63: 434-444. https://doi.org/10.1016/j.ijheatmasstransfer.2013.04.001.
14. **Jiang, B.; Yan, Sh.; Zhang, L.; Xiao, X.** 2017. Numerical research of stream analysis on helical baffles heat exchangers, J. Eng. Thermophys. 26(2): 272–290. https://doi.org/10.1134/S1810232817020102.
15. **Palen, J. W.; Taborek, J.** 1969. Solution of shell-side flow pressure drop and heat transfer by stream analysis method, Chem. Eng. Prog. Symp. Ser. 92 (65): 53-63.
16. **Schlunder, E. U.** 1983. Heat exchanger design handbook 1, 1st edn, Hemisphere Pub. Corp.
17. **Kuppan, T.** 2000. Heat exchanger design handbook, Marcel Dekker Inc.
18. **Saeedan, M.; Bahiraei, M.** 2015. Effects of geometrical parameters on hydrothermal characteristics of shell-and-tube heat exchanger with helical baffles: numerical investigation, modeling and optimization, Chem. Eng. Res. Des. 96: 43-53. https://doi.org/10.1016/j.cherd.2015.02.004.
19. **Zhang, J. F.; He, Y. L.; Tao, W. Q.** 2010. A design and rating method for shell-and-tube heat exchangers with helical baffles, J. Heat Transf. 132(05): 1801-1808. https://doi.org/10.1115/1.4000457.

M. Yousfi

HELICAL BAFFLE THERMOHYDRAULIC PERFORMANCE VERSUS SEGMENTAL BAFFLE ONE

S u m m a r y

In this contribution, we reworked the Bell-Delaware technique for a HB-STHX to systematically study its thermohydraulic performance behavior in the shell side. The helical baffles were continuous quadrant sectors exanimated for five inclination angles 25°, 30°, 35°, 40° and 45° at six different values of mass flow rate ranged from 10 kg/s up to 30 kg/s. We observed a clear increase in global heat transfer coefficient and a clear decrease in pressure loss, in continuous helical baffle case compared to segmental one when mass flow rate varied. The global heat transfer coefficient was positively correlated with Reynolds number and with the helix angle as 45° displayed the highest coefficient at 30 kg/s. We had a negative correlation between pressure loss and mass flow rate, and when helix angle increased we got a sort of quadratic variation, thus the baffle inclination of 45° followed by 25° provided still the least detrimental pressure drops at 10 kg/s. When Reynolds number raised, the performance evaluation factor fell, the latter had a somehow parabolic profile on helix angle: it was 45° followed by 25 who showed the most favorable ratio at 10 kg/s.

Keywords: overall heat transfer coefficient, pressure drop, continuous helical baffle, shell-and-tubes heat exchanger, Bell-Delaware method, correction factors.

Received April 16, 2022
Accepted November 28, 2022